

W-BAND FERRITE - DIELECTRIC IMAGE-LINE  
FIELD DISPLACEMENT ISOLATORS

J.M. Owens\*  
J.Y. Guo  
W.A. Davis  
R.L. Carter

The center for Advanced Electron Devices and Systems The University of  
Texas at Arlington, Arlington Texas

ABSTRACT

This paper describes the results of theoretical and experimental studies of image line field displacement isolators operating at W band (90-100 Ghz). Isolators were fabricated using gadolinium gallium garnet, and GaAs as the dielectric and Trans-Tech TT2-111 Nickel-Zinc Ferrite and Epitaxial Yttrium Iron Garnet as the non-reciprocal medium. Isolators with  $S_{21}-S_{12}$  ratios of greater than 20db have been designed, fabricated and tested.

INTRODUCTION

Ferrite isolators of the Faraday rotation, resonance or field displacement type, are widely used in metal wave guide circuits to over 200 Ghz. While these devices perform well in the millimeter range, they do not lend themselves to integration and low cost production. Dielectric image line is an attractive alternative technology at mm wave frequencies, since it can be produced by lithographic techniques applied to high-quality insulators as well as semi-insulating semi-conductors. The concept of a dielectric waveguide isolator was explored by Nanda (1) at V band with good results.

This paper describes the results of theoretical analysis of a simplified parallel plane waveguide model of a field displacement isolator. Although, this model was limited to consideration of the fundamental mode only. The model gave a clear picture of the forward and reverse propagation characteristics and allowed for the optimization of the design of the isolator. Experimental measurements were carried out on a range of structures utilizing a Millimeter Wave Vector Network Analyzer operating at 90-100 Ghz.

THEORY

The exact theoretical analysis of a dielectric image line displacement isolator is complex due to the anisotropy of the ferrite and the asymmetry of the physical configuration.

The theoretical analysis utilized for this study was based on the multislab parallel-plane waveguide model shown in Fig. 1 [2] [3]. Only the TE modes are assumed to exist. In this model slabs of different width, each with a different permittivity  $\epsilon$  and permeability tensor  $\langle\mu\rangle$  can be chosen. Conducting plates are at both the top and the bottom, while resistive regions are at both ends, thus representing either ground planes or absorbers. The boundary conditions at the interfaces are continuity of both tangential E and H. The propagation constants associated with propagation into the page are the same for all slabs. The materials are lossless, except for the loss in the absorbers. The permeability tensor for ferrite takes the form:

$$\langle\mu\rangle = \mu_0 \begin{bmatrix} \mu - jk & 0 \\ jk & \mu & 0 \\ 0 & 0 & 1 \end{bmatrix}$$

The solution for the fields in the slabs involves assuming solutions for each slab, matching boundary conditions, and solving the resulting set of complex variable nonlinear equations by the Newton-Raphson method.

Figure 2 shows a plot for the forward and reverse propagation fields for this structure with a biased ferrite. This model was used to both design and optimize the test isolators.

Using this model to optimize a structure with  $H_0 = 25,000$  gauss,  $f_0 = 95\text{GHz}$ , and  $4\pi\mu_m = 5000$  gauss, we found that  $2a_1 = 90\Omega\text{cm}$ , the ratio of forward to reverse attenuation,  $\alpha_R/\alpha_F$  was found to be 1.45 db/mm.

#### EXPERIMENTAL RESULTS

Characteristics of the biased ferrite-dielectric image line isolators were measured using a Hughes S-parameter test system shown in Figure 3. The measurement set-up utilized a modified section of W band waveguide with .75" of the sidewalls and top removed and the remaining bottom of the guide serving as the ground plane for the dielectric image guide. The structure is shown in Figure 4. The structure to be tested was fitted into the open ends of the guide, and a taper on the dielectric structure was used to match from the metal guide to the image guide. The angle for the optimum taper was found experimentally to be 60°. Devices were tested with the ferrite both parallel and perpendicular to the ground plane. As indicated by theory, the parallel configuration proved to be the best. The primary dielectric utilized in the experiments was gadolinium gallium garnet; a low loss single crystal material with relative dielectric constant of 16, Cr doped semi-insulating GaAs was also investigated. The primary ferrite used was Trans Tech TT2-111 Nickel-Zinc Ferrite, epitaxial YIG was also investigated. With care, the insertion loss of the image guide (no ferrite) alone can be as low as 2.5db, which is primarily loss in the waveguide to image guide transitions. Figure 5 shows  $S_{21}$  and  $S_{12}$  of an image line field displacement isolator with a 120Ωcm silicon absorber, a 250mm thick TT2-111 ferrite layer and a 500mm GGG guide as a function of absorber spacing. The device shows isolation ratios of greater than 20db from 91-93 GHz, and greater than 15db from 90-94GHz. Experiments with 25μm YIG has shown lower isolation ratios and narrower bandwidths. Experiments with GaAs as a

dielectric show similar isolation ratios and bandwidths, but higher total insertion losses (3-5db higher). It is believed that the increased insertion loss is the result of non optimum input/output match from the metal wave guide to the dielectric guide and increased propagation loss in the GaAs, which can be reduced by better material selection.

#### CONCLUSIONS

An image line field displacement isolator has been demonstrated at w-band which has good isolation characteristics and an insertion loss of as low as 2.5db. The device, as with many mm-wave devices could profit from materials with higher magnetization which would both reduce the bias field requirement and increase the bandwidth. The device has the potential for integration and mass production through the use of ridge guide structures on GaAs substrates and thus may be attractive for mm wave systems.

1) V.P. Nanda, "IEEE Trans MTT, Vol. MTT-24; pp 874-879 (1976).

2) Ramo, Whinnery, Vanduzer Fields and Waves in Communication Electronics, J. Wiley and Sons, 1984 pp 393-396.

3) M Hines, "IEEE Trans Microwave Theory and Tech., Vol. MTT-19; May 1971.

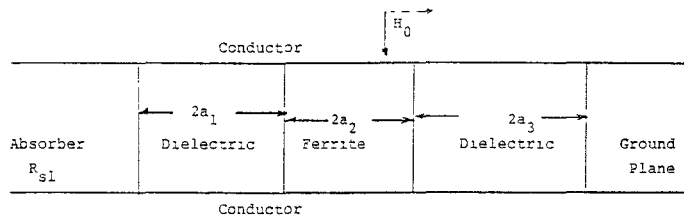


Figure 1: Multi slab parallel-plane waveguide model.

2a (mm)	0.06	0.14	0.30
$4\pi M_s$ (kGs)	0.00	5.00	0.00
$\epsilon_r$	16.00	12.00	16.00
$\alpha_x$ (/mm)	0.58	0.75	0.58
$\beta_x$ (/mm)	-7.54	-5.53	-7.54

Rs1	GGG	TT2	GGG	Rs2
30 $\Omega\text{-cm}$			1 $\Omega\text{-cm}$	

2a (mm)	0.06	0.14	0.30
$4\pi M_s$ (kGs)	0.00	5.00	0.00
$\epsilon_r$	16.00	12.00	16.00
$\alpha_x$ (/mm)	0.58	0.92	0.58
$\beta_x$ (/mm)	-6.45	-3.93	-6.45

Rs1	GGG	TT2	GGG	Rs2
30 $\Omega\text{-cm}$			1 $\Omega\text{-cm}$	

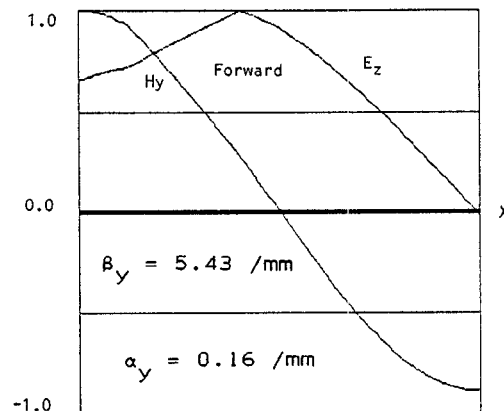
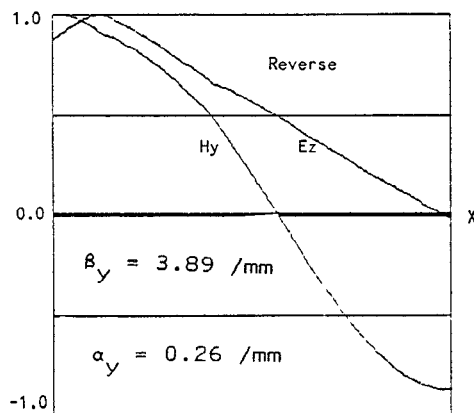
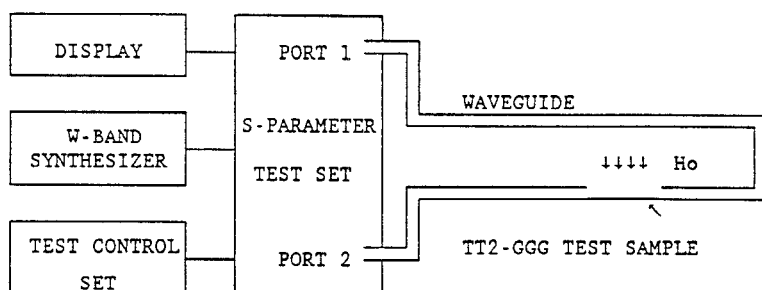


Figure 2: Calculated field components at 95.0 GHz with magnetic bias of 25 KG.



Display . . . . . HP8410, HP8412  
 W-band Synthesizer . . . HUGHES 4785  
 Test Control Unit . . . HUGHES 786H.5000  
 S-parameter Test Set . . . HUGHES 4786HX

Figure 3: S parameter test system.

## W-BAND FERRITE-DIELECTRIC IMAGE-LINE FIELD DISPLACEMENT ISOLATORS

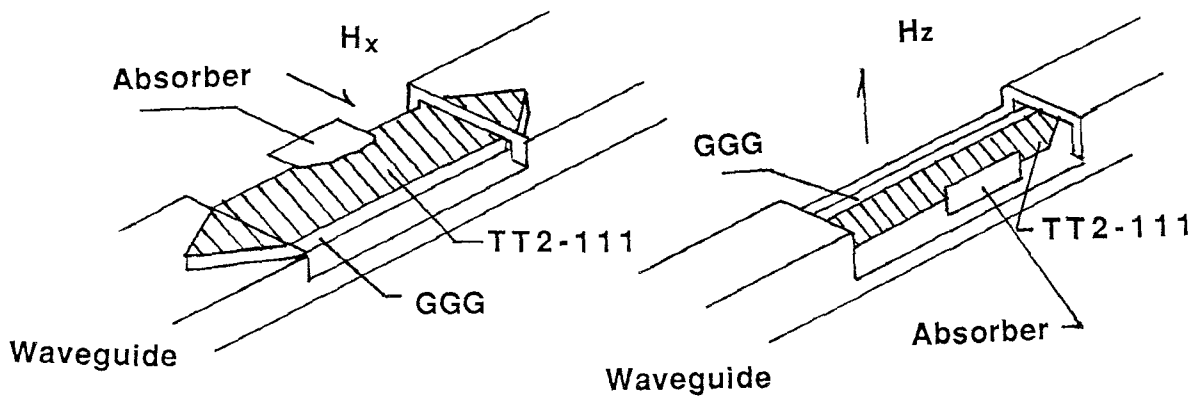


Figure 4: YIG or TT2-111 loaded wave-guide with the sample in the H-plane (left) or E-plane (right).

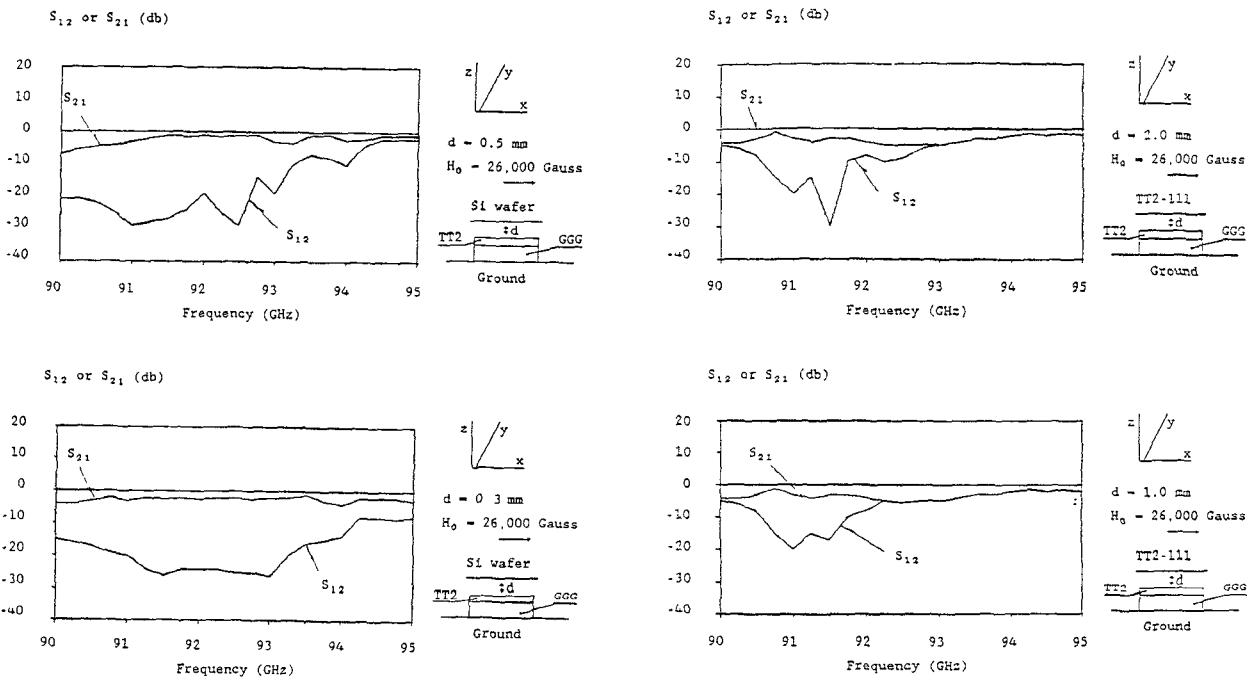


Figure 5:  $S_{12}$  and  $S_{21}$  for an image line with a silicon wafer as an absorber at different spacings.